Joint Pathology Center
Veterinary Pathology Services

WEDNESDAY SLIDE CONFERENCE 2022-2023

Conference #19 **8 February 2023**

CASE I:

Signalment:
10-year-old intact male French Bulldog (*Canis familiaris*)

History:
A 10-year-old intact male French Bulldog presented for evaluation of a left cranial cervical mass. One month prior to presentation, the dog was seen by his family veterinarian for weight loss and increased respiratory efforts. A complete blood count and serum biochemical profile were unremarkable. Thoracic radiographs revealed a marked diffuse bronchointerstitial pattern that was interpreted to be pneumonia and a course of antibiotics (doxycycline) was started. The clinical signs worsened, and three weeks later the dog presented to an internal medicine service with coughing, gagging, shallow breathing, and reduced appetite. A nonmobile firm mass in the left craniolateral cervical region near the mandibular angle was palpated; a computed tomography (CT) scan revealed a heterogeneous, contrast enhancing mass that compressed the larynx medially. Cytology of a fine needle aspiration of the mass was diagnostic for neoplasia, and highly suggestive of an epithelial tumor.

On presentation, the dog was bright and alert and mildly overweight (body condition score, 3.5/5). On physical examination, the dog had laborious breathing with increased abdominal effort and increased upper respiratory sounds. The rest of the physical examination and the cardiac auscultation were unremarkable. The dog underwent a head/thorax CT the next day. The CT revealed a diffuse nodular pattern in the lungs, consistent with pulmonary metastases. The cervical mass was interpreted as an enlarged left medial retropharyngeal lymph node, and multiple tracheobronchial, sternal, mediastinal and cervical lymph nodes were rounded. The changes were diagnosed as carcinoma metastases, origin of primary mass uncertain, and the owners elected for human euthanasia.

Gross Pathology:
On gross post-mortem examination, intimately adherent to the outer wall of the left common carotid artery at the bifurcation into the external and internal carotid arteries, was a 3 cm in diameter firm, tan/white nodular mass that was soft to firm and mottled red/white on cut section. Another mass of

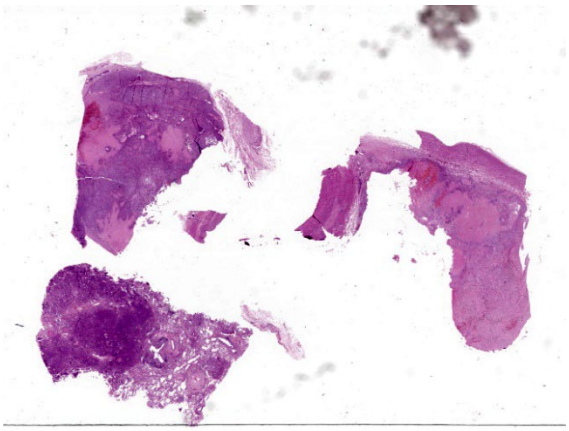

Figure 1-1. Lung, mediastinum, dog. Two sections of mediastinum (top) and one section of lung (bottom left) are submitted for examination. (HE, 5X)

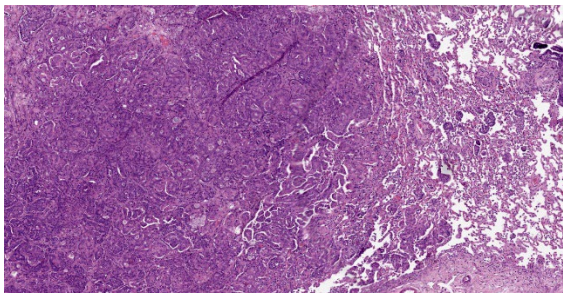

Figure 1-2. Lung, dog. An infiltrative neoplasm is present within the lung and extends into adjacent alveoli. (HE, 66X)

similar size and appearance was identified intimately adherent to the outer wall of the aorta at the heart base. Throughout the parenchyma of the lungs were generalized firm, white to grey nodules, some of which were raised by up to 5 mm, that varied in size from 0.3 to 2.5 cm in diameter, affecting all lung lobes equally and representing approximately 75% of the lungs. Multiple bronchial, cervical, and pancreatic lymph nodes were up to 2 times enlarged and homogeneously pale tan on cut surface. Other gross abnormalities included a 2 mm in diameter, firm, tan focus within the parenchyma of the right testis.

Laboratory Results:
No laboratory findings reported.

Microscopic Description:
Within the connective tissue surrounding the tunica adventitia of the external and internal carotid arteries, is a partially encapsulated, focally infiltrative multilobular neoplastic mass. The mass was predominantly (50%) composed of lobules of polygonal cells separated by dense bands of connective tissue and arranged in nests and packets separated by a fine highly vascular stroma. Neoplastic cells had variably distinct borders, a moderate amount of frequently wispy granular cytoplasm, and a round to oval nucleus with coarsely granular chromatin. There was occasionally karyomegaly (up to 8 times) and rare mitotic figures.

Additionally, multifocally throughout the mass, clusters of neoplastic cells sometimes in a tubular pattern, and represented approximately 30% of the section. These regions have a different cell morphology; cuboidal neoplastic cells with distinct cell borders, moderate amounts of cytoplasm and condensed chromatin were arranged in cords and tubules, sometimes with intraluminal wispy basophilic material. In these areas, there were 11 mitotic figures per 10 high power fields (HPF). The remainder of the mass (20%) was composed of coalescing areas of necrosis, characterized by loss of tissue architecture and replacement by eosinophilic cellular debris. The aortic mass had a similar mixed morphological appearance, but with larger areas (70%) of necrosis.

Within the pulmonary parenchyma, compressing and replacing lung tissue, were multiple poorly circumscribed, infiltrative nodules of neoplastic epithelial cells that are arranged in cords and tubules that sometimes contained necrotic debris, supported and moderate stroma. The cells were cuboidal to columnar, sometimes ciliated, with distinct cell borders, abundant eosinophilic cytoplasm, and a round to oval nucleus with condensed chromatin. There was 2-fold anisocytosis and anisokaryosis and 14 mitotic figures per 10 HPF. Neoplastic cells similar to the ones described in the lung were also found effacing bronchial and pancreatic lymph

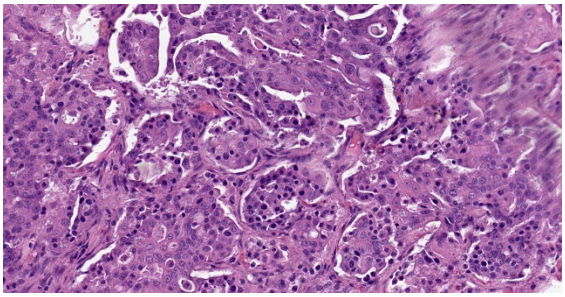

Figure 1-3. Lung, dog. Neoplastic cells are cuboidal to columnar and forms tubules and papillary projections in adjacent alveolar spaces. (HE, 346X)

nodes, and within lumen of blood and/or lymphatic vessels surrounding lungs, aorta, pancreas, and adrenal glands.

Other histological abnormalities included an interstitial cell tumor in the right testis. The cervical lymph nodes were hyperplastic and draining hemorrhage, but no neoplastic cells were present.

Representative sections from the carotid body tumor, the aortic body tumor, a pulmonary adenocarcinoma nodule, and a bronchial lymph node with metastasis were stained for chromogranin A (rabbit polyclonal, dilution 1:400, Dako, Glostrup, Denmark; labels approximately 65% of canine chemodectomas4,9,21), synaptophysin (rabbit monoclonal, ready to use, Ventana Medical Systems, Tucson, USA; labels 65% of canine chemodectomas4), pan-cytokeratin (mouse monoclonal, clone AE1/AE3, dilution 1:100, Dako, Glostrup, Denmark; labels 100% of canine primary pulmonary epithelial tumors [9]), and thyroid transcription factor-1 (TTF-1) (mouse monoclonal, clone 8G7G3/1, dilution 1:50, Dako, Glostrup, Denmark; labels 85% of canine primary pulmonary tumours2). External positive controls for IHC were pancreas, thyroid gland, and parathyroid gland for chromogranin A; pancreas, brain, adrenal gland and thyroid gland for synaptophysin; lung, liver, kidney, and small intestine for pan-cytokeratin; and thyroid gland for TTF-1. Slides incubated with non-immune rabbit serum or with antibody diluent were used as negative controls.

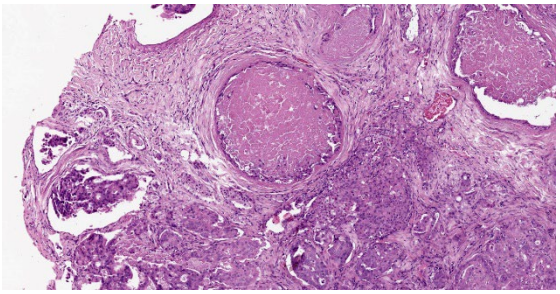

Figure 1-4. Lung, dog. There is lymphovascular invasion of pulmonary vessels and lymphatics by neoplastic cells. Some lymphatic emboli are necrotic. (HE, 200X)

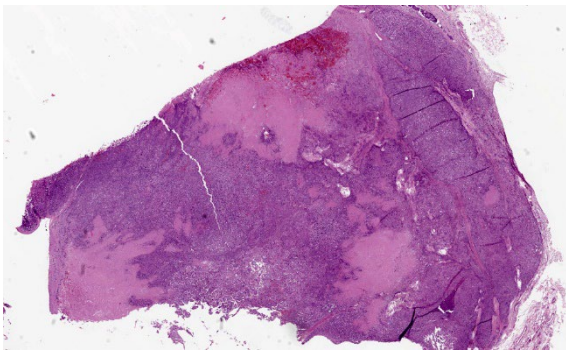

Figure 1-5. Mediastinum, dog. A second, partially necrotic neoplasm effaces mediastinal tissue. (HE, 14X)

The nests of polygonal neoplastic cells showed intense diffuse cytoplasmic immunoreactivity for chromogranin A and synaptophysin in the carotid body and aortic body tumors, while tubule-forming cuboidal neoplastic cells in the chemodectomas, and pulmonary and lymph node neoplastic cells were negative. The neoplastic epithelial cells within the lung and bronchial lymph node, and the tubule-forming cuboidal neoplastic cells in the carotid body and aortic body tumors showed weak to moderate diffuse cytoplasmic and weak to intense membranous immunoreactivity for pan-cytokeratin, while the nests of polygonal cells in the chemodectomas were negative. Immunoreactivity for TTF-1 was negative in all neoplastic cells examined; intense nuclear staining was observed in occasional type II pneumocytes (internal positive control).

Contributor's Morphologic Diagnoses:
Carotid body tumor
Aortic body tumor
Pulmonary adenocarcinoma with metastases to lung, carotid and aortic body tumors, and bronchial and pancreatic lymph nodes

Contributor's Comment:
Based on the locations of the cervical and aortic masses, a preliminary diagnosis of ca-

rotid body and aortic body tumors with metastases to the lungs was made; representative sections of the masses and internal organs were fixed in 10% neutral buffered formalin and processed for histopathological examination. It is also worth noting that the dog is a brachycephalic breed (French bulldog), and chemodectomas have been shown to occur at a higher frequency in brachycephalic breeds such as Boxers, Bulldogs, and Boston Terriers, predominantly in middle-aged to older males.[10,11,16,22] Aortic body tumors are diagnosed 4 to 12 times more often than carotid body tumors in dogs, and multiple chemodectomas are not uncommon, with 14-22% of dogs with carotid body tumors having a concomitant aortic body tumour.[10,11,12, 16,22]

The pulmonary masses were diagnosed as a primary pulmonary adenocarcinoma with metastases to bronchial and pancreatic lymph nodes. Given the two histologically distinct areas within the carotid body and aortic body tumors, immunohistochemistry (IHC) was done to further characterize the neoplasm. Representative sections from the carotid body tumor, the aortic body tumor, a pulmonary adenocarcinoma nodule, and a bronchial lymph node with metastasis were stained for chromogranin A, synaptophysin, pan- cytokeratin, and thyroid transcription factor-1 (TTF-1). (See microscopic description for IHC results). The IHC findings, together with the gross observations, were interpreted as a primary pulmonary acinar adenocarcinoma with metastases to carotid and aortic body tumors, and bronchial and pancreatic lymph nodes. It should be noted, however, that a primary carcinoma of unknown origin with metastases to lung and other tissues could not be ruled out.

Tumor-to-tumor metastasis is a rare phenomenon, with only about 100 human cases reported in the English literature.[14] To the best of our knowledge, this has only been reported

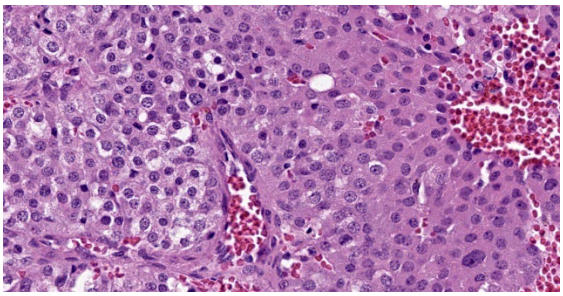

Figure 1-6. Mediastinum, dog. Neoplastic cells are polygonal, arranged in nests and packets, with finely granular to clear cytoplasm, and there is moderate anisokaryosis (bottom right). (HE, 574X)

once in a domestic species; a dog with a mammary gland tumor that metastasized to a right auricular haemangiosarcoma.[13] Tumor-to-tumor metastasis should not be confused with a "collision tumor". The term "collision tumor" refers to two histologically distinct, proximally coexistent, but independent tumors. Criteria have been suggested to define a tumor-to-tumor metastasis, which include the presence of more than one primary tumor, and that the metastatic (or donor) neoplasm is a true metastasis rather than contiguous growth of two tumors (i.e., collision tumor) or embolization of tumor cells without established growth.[7]

In humans, the most frequent donors are lung and breast carcinomas, while the most frequent recipients are renal cell carcinomas, sarcomas, and meningiomas.[17] In general, recipient tumors are slow growing, well vascularized, and can vary from benign to highly malignant. Pulmonary carcinomas have been reported to metastasize to several different types of tumours,[6] with most reported cases metastasizing to renal cell carcinomas[19] and intracranial meningiomas.[3] There are two reports of tumor metastasis to chemodectomas; one intracranial chemodectoma with metastasis from an esophageal carcinoma[15], and a carotid body tumor with metastasis from a poorly-differentiated pulmonary carcinoma.[6]

Concurrent primary neoplasms are not infrequent in dogs with chemodectomas. An investigation into 357 cases of dogs with chemodectomas found that 38% had at least one other microscopically confirmed primary tumour.[10] The most frequent second primary tumors were thyroid carcinomas and interstitial cell tumors. Pulmonary carcinoma, seen in 6 dogs, was the 11th most frequent second primary tumor. There are several possible reasons for the co-occurrence of chemodectomas and second primary tumors. Chemodectomas metastasize infrequently (12-22% of cases), are usually slow growing, non-functional and generally found in older dogs where they can act as space-occupying lesions.[10,16] Therefore, dogs diagnosed with chemodectomas simply have an extended time in which to develop a second primary tumor. There could also be a genetic component, with dogs genetically predisposed to chemodectomas also being at higher risk for other tumors. Indeed, bulldog-related breeds had a higher number of second primary tumors (47%) compared to all other breeds (32%).[10]

Contributing Institution:
University of Guelph
Guelph, Ontario Canada
www.uoguelph.ca

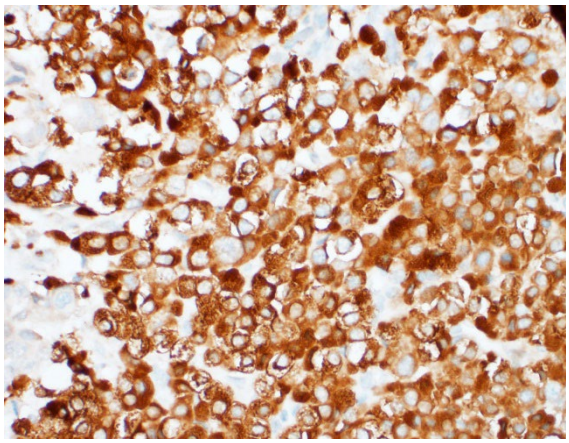

Figure 1-7. Mediastinum, dog. Neoplastic cells are strongly positive for chromogranin A. (anti Chroma-granin-A, 400X)

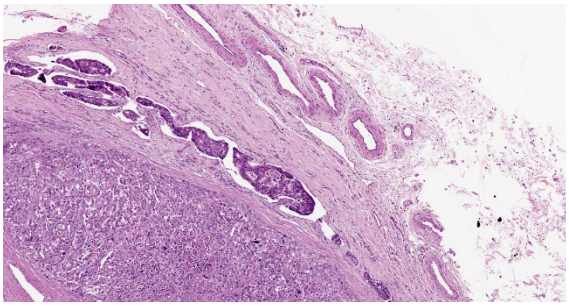

Figure 1-8. Mediastinum, dog. Metastatic cells from the pulmonary carcinoma are present in lymphatics at the periphery of the chemodectoma. (HE, 79X)

JPC Diagnosis:
1. Lung: Pulmonary adenocarcinoma.
2. Fibrovascular tissue (presumed mediastinum) (2): Neuroendocrine carcinoma and metastatic pulmonary adenocarcinoma.

JPC Comment:
This week's moderator, Colonel (Retired) Jo Lynne Raymond, and conference participants discussed whether the adenocarcinoma could be definitively diagnosed as pulmonary adenocarcinoma based on H&E. Conference participants felt the variable patterns of growth, including tubular, acinar, and lepidic patterns, and few visible cilia along the apical aspect of neoplastic cells are strongly suggestive of pulmonary origin.

Pulmonary adenocarcinomas are the most common lung tumor in dogs. Patterns of tumor growth include minimally invasive, lepidic, papillary, acinar, solid, and micropapillary, and the predominant histologic pattern can be predictive of biologic behavior.[8] The first three are the most commonly reported in dogs and have the longest survival times.[8] In the lepidic pattern, neoplastic cells form single-cell layer linings which trace alveolar walls, akin to a row of butterflies resting on a branch.[18] Papillary growths are more cellular than the lepidic pattern, and form exophytic projections into alveolar lumens.[20] In the acinar form, neoplastic cells line tubules and chords.[20] Pulmonary carcinomas may

also form squamous or adenosquamous patterns, with the latter being composed of at least 10% glandular and 10% squamous populations.[18]

In cats, tumor size is correlated with rate of metastasis[8], a finding which was confirmed in a recent retrospective study by Santos et al which described gross and histologic features of pulmonary carcinomas in 39 cats.[18] Tumors larger than 1.9 cm in diameter were more likely to metastasize. While metastasis to the digit has traditionally been the most well recognized in cats[8], this study found metastasis to the skeletal muscle, kidneys, and parietal pleura more common than digital metastasis, reinforcing the use of the MODAL acronym (muscle, ocular, digit, aorta, lung).[18] Additionally, the authors found that pulmonary carcinomas were the cause of death in only 66% of cases; cats frequently had comorbidities related to old age (lymphoma, chronic renal disease) which contributed to mortality.[18]

The study also evaluated P-40 and napsin-A expression in feline pulmonary carcinomas. Nuclear P-40 expression was found in all of the adenosquamous variants (with immunoreactivity in 100% of squamous cells and approximately 30% of the glandular components), which is expected for this basal cell marker expressed in cutaneous squamous cell carcinomas.[18] Napsin-A, on the other hand, was non-contributory in all feline tissues.[18] Napsin A is used in evaluation of human pulmonary tumors and has some utility in canine pulmonary carcinomas: another recent study showed Napsin A expression in 62 of 67 canine pulmonary adenocarcinomas.[1] The specificity is relatively low, however, as it is expressed in 60% of thyroid neoplasms and renal cell carcinomas, which are important differentials to consider for any carcinoma in the lung.[1]

References:

1. Beck J, Miller MA, Frank C, DuSold D, Ramos-Vara JA. Surfactant Protein A and Napsin A in the Immunohistochemical Characterization of Canine Pulmonary Carcinomas: Comparison with Thyroid Transcription Factor I. *Vet Pathol*. 2017; 54(5): 767-774.
2. Bettini G, Marconato L, Morini M, Ferrari F. Thyroid transcription factor-1 immunohistochemistry: diagnostic tool and malignancy marker in canine malignant lung tumours. *Vet Comp Oncol*. 2009; 7: 28-37.
3. Bhargava P, McGrail KM, Manz HJ, Baidas S. Lung carcinoma presenting as metastasis to intracranial meningioma: case report and review of the literature. *Am J Clin Oncol*. 1999; 22: 199-202.
4. Brown PJ, Rema A, Gartner F. Immunohistochemical characteristics of canine aortic and carotid body tumours. *J Vet Med A Physiol Pathol Clin Med*. 2003; 50: 140-144.
5. Burgess HJ, Kerr ME. Cytokeratin and vimentin co-expression in 21 canine primary pulmonary epithelial neoplasms. *J Vet Diagn Invest*. 2009; 21: 815-20.
6. Bury Y, Green R, Jain M, Moor J. Metastasis of carcinoma of the lung to a carotid body paraganglioma. *BMJ Case Rep*. 2012.
7. Campbell LV Jr, Gilbert E, Chamberlain CR Jr., Watne AL. Metastases of cancer to cancer. *Cancer*. 1968; 22: 635-643.
8. Caswell JL, Williams KJ. Respiratory System. In: Maxie MG, ed. *Jubb, Kennedy, and Palmer's Pathology of Domestic Animals*. Vol 2. 6th ed. St. Louis, MO: Elsevier. 2017; 495-496.

9. Doss JC, Grone A, Capen CC, Rosol, TJ. Immunohistochemical localization of chromogranin A in endocrine tissues and endocrine tumors of dogs. *Vet Pathol*. 1998; 35: 312-5.
10. Hayes HM, Sass B. Chemoreceptor neoplasia: a study of the epidemiological features of 357 canine cases. *Zentralbl Veterinarmed A*. 1988; 35: 401-408.
11. Hayes HM. An hypothesis for the aetiology of canine chemoreceptor system neoplasms, based upon an epidemiological study of 73 cases among hospital patients. *J Small Anim Pract*. 1975; 16: 337-43.
12. Hayes HM Jr., Fraumeni JF Jr. Chemodectomas in dogs: epidemiologic comparisons with man. *J Natl Cancer Inst*. 1974; 52, 1455-1458.
13. Hilbe M, Hauser B, Zlinszky K, Ehrensperger F. Haemangiosarcoma with a metastasis of a malignant mixed mammary gland tumour in a dog. *J Vet Med A Physiol Pathol Clin Med*. 2002; 49: 443-444.
14. Lee T, Cha YJ, Ahn S, Han J, Shim YM. A Rare Case of Tumor-to- Tumor Metastasis of Thyroid Papillary Carcinoma within a Pulmonary Adenocarcinoma. *J Pathol Transl Med.* 2015; 49: 78-80.
15. Lu JQ, Khalil M, Hu W, Sutherland GR, Clark AW. Tumor-to-tumor metastasis: esophageal carcinoma metastatic to an intracranial paraganglioma. *J Neurosurg*. 2009; 110: 744-8.
16. Patnaik AK, Liu SK, Hurvitz AI, McClelland AJ. Canine chemodectoma (extra-adrenal paragangliomas) - a comparative study. *J Small Anim Pract*. 1975; 16: 785-801.
17. Petraki C, Vaslamatzis M, Argyrakos T, et al. Tumor to tumor metastasis: report of two cases and review of the literature. *Int J Surg Pathol*. 2003; 11: 127-35.
18. Santos IR, Raiter J, Lamego EC, et al. Feline pulmonary carcinoma: Gross, histological, metastatic, and immunohistochemical aspects. *Vet Pathol.* 2023; 60(1):8-20.
19. Sella A, Ro JY. Renal cell cancer: best recipient of tumor-to-tumor metastasis. *Urology*. 1987: 30; 35-8.
20. Wilson DW. *Tumors of the Respiratory Tract*. In: Meuten DJ, ed. Tumors of Domestic Animals. Ames, IO: Wiley Blackwell. 2017; 487-490.
21. Yamamoto S, Fukushima R, Hirakawa A, Abe M, Kobayashi M, Machida N. Histopathological and immunohistochemical evaluation of malignant potential in canine aortic body tumours. *J Comp Pathol*. 2013; 149: 182-191.
22. Yates WD, Lester SJ, Mills JH. Chemoreceptor tumors diagnosed at the Western College of Veterinary Medicine 1967-1979. *Can Vet J*. 1980; 21: 124-129.

CASE II:

Signalment:
9-year-old, castrated male, Netherland dwarf rabbit (*Oryctolagus cuniculus domesticus)*

History:
This rabbit presented to the rDVM with chronic uveitis which was poorly responsive to treatment with oral and topical non-steroidal anti-inflammatory drugs and antibiotics. The rabbit otherwise appeared to be in good health. The owners opted for enucleation and submission for of the eye for histopathology.

Gross Pathology:
The submitted eye was grossly unremarkable.

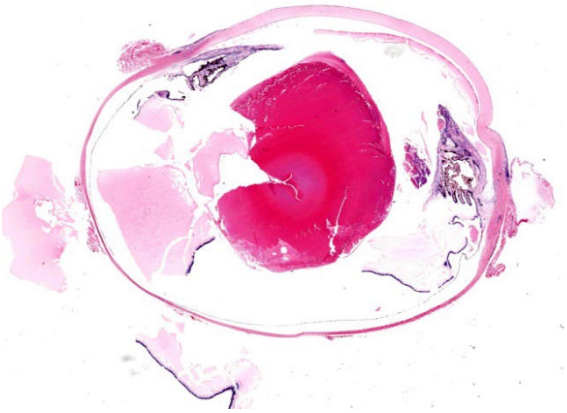

Figure 2-1. Globe, dwarf rabbit. A globe is presented for examination. The cornea is at top. There are areas of pallor within the lens, and eosinophilic protein within the posterior segment. (HE, 6X)

Laboratory Results:
No laboratory findings reported.

Microscopic Description:
The iris contains moderate diffuse infiltrates of plasma cells accompanied by small numbers of lymphocytes and few scattered heterophils. Occasional strands of fine fibrous stroma associated with moderate aggregates of epithelioid macrophages, fewer multinucleated giant cells, occasional heterophils, proteinaceous debris and a few erythrocytes are noted in the anterior and posterior chambers. Thin strands of fibrous tissue rarely extend from the posterior iris near the pupillary margin. There are large areas where subcapsular lens fibers appear fragmented, rounded and are replaced by amorphous pink debris. Small amounts of basophilic, fine mineral, as well as numerous, 1-2 micron long, ovoid, gram positive, spores, are present beneath the lens capsule and within lens epithelial cells. Lens epithelial cells are often vacuolated and rarely form small piled up aggregates. In some areas, subcapsular lens fibers are lost and replaced by sparse cell debris.

Contributor's Morphologic Diagnoses:
Eye: Moderate, chronic, plasmacytic and granulomatous, anterior uveitis with cataracts and numerous intralenticular, gram positive, microsporidial spores (consistent with Encephalitozoon cuniculi)

Contributor's Comment:
The clinical history and microscopic appearance of the ocular lesions in this rabbit are most compatible with cataract formation and phacoclastic uveitis due to the ocular form of *Encephalitozoon cuniculi* infection.

Encephalitozoon cuniculi is a microsporidial pathogen with worldwide distribution. Although previously phylogenetically classified as a protozoa, it is currently considered a fungus.[5,6] There are three major genotypes of *E. cuniculi*. Genotype 1 (or the rabbit strain) is generally associated with disease in pet and commercially raised rabbits. This organism has a direct life cycle. Horizontal transmission is most commonly through the ingestion of spores in urine-contaminated feed, or less commonly via inhalation. Vertical (or transplacental) transmission may also occur and is often hypothesized to be the cause of intraocular infections which facilitates access to, and colonization of lens fibers during fetal development.[6] Typically, in the intestine, the spores primarily infect host cells through extrusion of their polar filament and injection of sporoplasm into a host cell. Phagocytosis

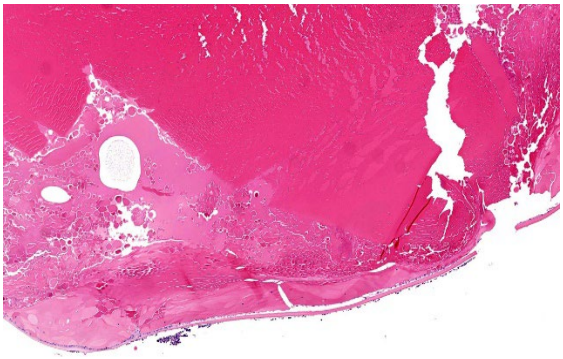

Figure 2-2. Globe, dwarf rabbit. There is degeneration of the posterior lens fibers with formation of Morgagnian globules. (HE, 66X)

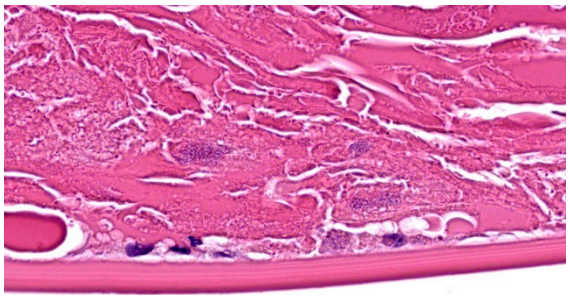

Figure 2-3. Globe, dwarf rabbit. In areas of degeneration, fibers are often swollen by cytoplasmic microsporidial spores. (HE, 857X)

by host cells has also been demonstrated.[6] Initial target organs for infection via horizontal transmission are those with high blood flow such as the lungs, liver and kidney but many sites may be involved. Infection of the central nervous system (CNS) generally occurs later in the course of disease. At tissue sites, sporogony continues and eventually leads to rupture of host cells and the release of spores which induces a localized lymphoplasmacytic to granulomatous inflammatory response. Most immunocompetent animals have subclinical infections with foci of granulomatous inflammation most commonly present in the brain, kidneys, and eye.[5,6] Spores are shed intermittently in the urine of infected rabbits. Clinical disease in rabbits is most often seen in older rabbits as immunocompetency wanes with age or following stressors that may have a negative impact on the host immune response (ie. changes in environment, other illnesses, medications, etc). In rabbits, the most common manifestations of *E. cuniculi* infection are clinical signs of central nervous system disease, uveitis, and chronic renal disease.

Rabbits with encephalitozoonosis most commonly present with a variety of neurologic clinical signs resulting from foci of lymphoplasmacytic to granulomatous meningoencephalitis. Many affected rabbits develop central vestibular disease which presents as head tilt, ataxia, nystagmus, and/or circling movements. More severe clinical signs may include rotation along the body length axis (i.e., rolling) or lateral recumbency which are generally associated with a poorer prognosis.[5] The main clinical differential diagnosis in these rabbits is peripheral vestibular disease due to otitis interna. Other neurologic signs that may be associated with encephalitozoonosis include seizures, paresis, altered mentation and behavioural changes.

Ocular lesions are most frequently reported in young rabbits with no other apparent clinical signs and lesions are most often unilateral. However, bilateral lesions have been documented in rabbits.[5] In some cases (likely largely older individuals), other clinical signs (especially neurologic signs) may also be noted.[8] In the eye, spores infect the lens epithelial cells and when these cells rupture it results in lens fiber degeneration, cataract formation and eventually phacoclastic uveitis.

Rabbits with significant renal disease resulting from chronic encephalitozoonosis often have slightly pale, pitted kidneys that microscopically exhibit lymphoplasmacytic to granulomatous, tubulointerstitial nephritis with fibrosis. These rabbits generally present with non-specific clinical signs of polyuria, polydipsia, weight loss, dehydration, and anorexia.

Figure 2-4. Globe, dwarf rabbit. A Gram stain demonstrates microsporidial spores within lens fibers. (Brown-Brenn, 400X)

In tissue sections, within foci of inflammation, microsporidial organisms are gram-positive which is a useful means of highlighting spores. Immunohistochemistry (IHC) and PCR testing of tissues, especially the eye contents, has been used to try to confirm a diagnosis of encephalitozoonosis. Unfortunately, PCR and IHC testing for diagnostic specimens is not easily accessible. Antemortem diagnosis of *E. cuniculi* remains a challenge. *Encephalitozoon cuniculi* is considered zoonotic, especially in immunocompromised people who are at an increased risk of acquiring infection.

Contributing Institution:
Atlantic Veterinary College, University of Prince Edward Island

JPC Diagnosis:
Eye, globe: Uveitis, phacoclastic, granulomatous, diffuse, moderate, with cataractous change and intralenticular microsporidial spores.

JPC Comment:
This is a classic case of phacoclastic uveitis caused by *E. cuniculi*. These microsporidian parasites have a characteristic coiled polar filament visible on electron microscopy as parallel strips winding around the nucleus, or if viewed in cross section, as regularly spaced circles along the periphery of the organism.[3] As the contributor mentioned, there are several genotypes of *E. cuniculi*, with genotypes II, III, and IV representing murine, canine, and human strains, respectively, though the genotypes are not exclusive to a single host species.[3] *E. cuniculi* can infect a variety of species, including guinea pigs, mice, rats, hamsters, primates, foxes, birds, dogs, and humans.[1,3] Ocular *E. cuniculi* infections have been sporadically documented in other species; for instance, cataracts have been reported in a snow leopard, dogs, mink, and blue foxes.

Two reports have described *E. cuniculi* cataracts in domestic cats in Austria and California. In a 2011 report by Benz et al, positive *E. cuniculi* titers were found in 11 cats (total of 19 eyes) with uveitis and cataracts in Austria.[2] In 18 of the eyes, *E. cuniculi* was identified on PCR of lens material.[2] In 11 of the eyes, histopathology with acid-fast trichrome of the anterior lens capsule revealed *E. cuniculi* spores in the lens epithelial cells.[2] The authors concluded that a positive *E. cuniculi* titer in conjunction with cataracts is strongly indicative of active infection in cats.[2] Similarly, *E. cuniculi* infection was diagnosed in three cats with immature cataracts and uveitis in California based on lens histopathology (hematoxylin and eosin or Ziehl-Neelsen) or PCR, and serologic testing was positive in the two tested cats.[7] These reports illustrate that *E. cuniculi* can induce similar ocular lesions in cats as in rabbits.

Control of the infection appears to be linked to the Th1 immune response and IFN-gamma production.[3] Studies have shown an initial CD4+ T-cell proliferation in the spleen followed by CD8+ T-cell proliferation, and high levels of IFN-gamma can be detected in the spleen, mesenteric lymph nodes, and Peyer's patches.[3] Humoral immunity does not appear to offer sufficient protection against infection

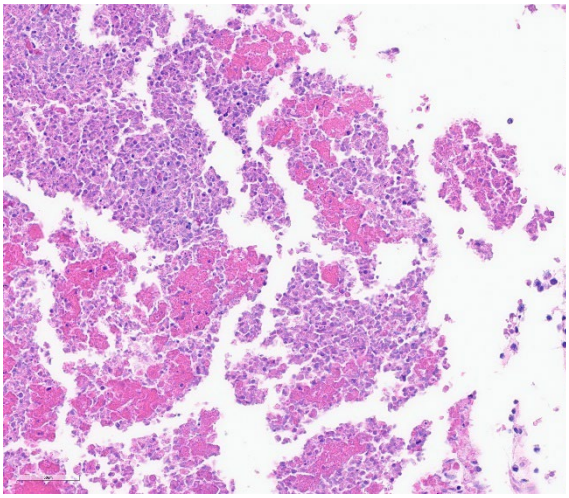

Figure 2-5. Globe, dwarf rabbit. There is extruded lens protein in the posterior chamber with aggregates of degenerate macrophages. (HE, 381X)

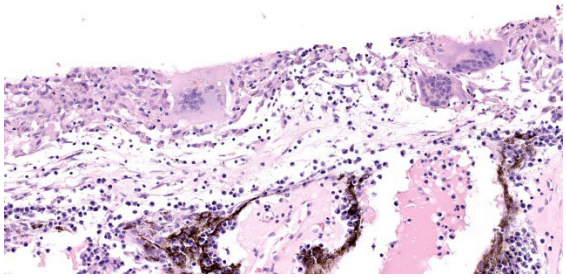

Figure 2-6. Globe, dwarf rabbit. The ciliary body is lined by a fibrovascular membrane lined by epithelioid macrophages and multinucleated giant cells. (HE, 246X)

but may aid in diagnosis as serologic testing is one of the few antemortem tests available.[3] Antibody titers initially rise by 4 weeks post infection and are high by 9 weeks.[1] Infected animals have an initial spike in IgM followed in a few weeks by an IgG spike.[3] Since a single positive titer cannot differentiate active infection from previous exposure, serial sampling to evaluate the titer differences is crucial. Perhaps the most helpful test is a negative titer: while a single negative test may happen in acute infections, paired negative titers spaced three weeks apart can rule out *E. cuniculi* infection.[3]

Spontaneous and congenital cataracts also occur in domestic rabbits and should be considered as a differential diagnosis for *E. cuniculi*-induced cataracts.[1] The incidence of cataracts in New Zealand white rabbits is suggestive of an inherited autosomal recessive defect in this breed.[1] As the contributor mentions, intra-ocular infection by *E. cuniculi* in rabbits is speculated to be due to in utero infection of the developing lens; however, a recent study in specific-pathogen free rabbits demonstrated lens after experimental oral infection with *E. cuniculi*, indicating other routes of infection may be possible.[4]

References:

1. Barthold SW, Griffey SM, Percy DH. *Pathology of Laboratory Rodents and Rabbits.* 4th ed. Ames, IO: John Wiley & Sons, Inc. 2016; 79, 146, 186, 234, 293-295, 318.
2. Benz P, Maas G, Csokai J, et a. Detection of *Encephalitozoon cuniculi* in the feline cataractous lens. *Vet Ophthalm.* 2011; 14 (Suppl 1) 37-47.
3. Dobosi AA, Bel LV, Pasitu AI, Pusta DL. A Reivew of *Encephalitozoon cuniculi* in Domestic Rabbits (*Oryctolagus cuniculus*)-Biology, Clinical Signs, Diagnostic Techniques, and Prevention. *Pathogens*. 2022; 11: 1486-1500.
4. Jeklova E, Leva L, Kummer V, Jekl V, Faldyna. Immunohistochemical Detection of *Encephalitozoon cuniculi* in Ocular Structures of Immunocompetent Rabbits. *Animals (Basel)*. 2019; 9(11): 988-995.
5. Kunzel F, Fisher PG. Clinical signs, diagnosis, and treatment of *Encephalitozoon culiculi* infection in rabbits. *Vet Clin Exot Anim.* 2018; 21:69-82.
6. Latney LV, Bradley CW, and Wyre NR. *Encephalitozoon cuniculi* in pet rabbits: diagnosis and optimal management. *Vet Med Res.* 2014; 5:169-180.
7. Lin J, Nell B, Horikawa T, Zarfoss. Feline intraleunticular *Encephalitozoon cuniculi:* three cases from California. *JFMS Open Rep.* 2022; 8(2): 1-9.
8. Morsy EA, Salem HM, Khattab MS, Hamza DA, and Abuowarda MM. *Encephalitozoon cuniculi* infection in farmed rabbits in Egypt. *Acta Vet Scand.* 2020; 62:11

CASE III:

Signalment:
13 Years, male, indoor only cat (*Felis catus)*

History:
The cat presented at the vet because the owner had realized that the right eye seemed "bigger", accompanied by a widened pupil. The clinical examination revealed normal pulse, mucosal surfaces, abdomen and lymph

nodes as well as nondescript auscultation of heart and lung.

The intraocular pressure in the right eye was 59 mm Hg initially, and the intraocular pressure was 25 mmHg in the left eye. After one week of treatment with Azopt three times per day, the intraocular pressure of the right eye was reduced to 21 mmHg at the second consultation.

Values of the clinical examination at the second consultation:
Blood pressure: 160/120 (5 measurements)
Glucose: 6.4 mmol/l
T4: within the normal range
Renal values: within the normal ranges

Clinical examination of the right eye: eye is open; reflexes are negative apart from a minimal pupil reflex; eye lids and their position are in within normal range; the conjunctiva is pink; the cornea is clear; the anterior eye chamber is clear; iris is in mydriasis; the lens demonstrates mild nucleosclerosis; the corpus vitreous with partly ablated retina in nasal area with a pigmented mass in the temporal area extending into the corpus vitreous.

Ultrasound of the right eye: temporal mass in the area of the ciliary body /periphery of the fundus lead to a suspicion of intraocular melanoma or mass of the ciliary body.

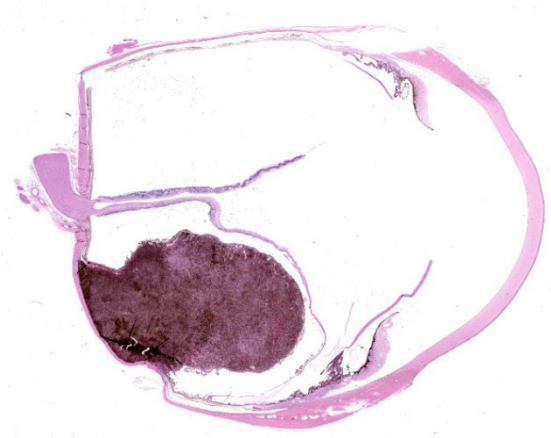

Figure 3-1. Globe, cat. A large, pigmented neoplasm arises from the subretinal choroid. The retina is detached and only a fragment of lens capsule is present in this section. (HE, 6X)

Two weeks after the first presentation, transpalpebral enucleation of the right eye with a continuous closure with Vicryl 5/0 suture material was performed. The suture material of the cutaneous suture was removed 10 days after surgery.

Gross Pathology:
Oculus dexter: Conjunctiva bulbi, cornea, anterior eye chamber, iridicorneal angle, iris, lens, ciliary body, the retinal pigment epithelium, the papilla nervi optici, n. opticus and the sclera did not show any macroscopical changes.

The vitreous was only partially present between a pigmented chorioidal mass and the completely ablated, cup shaped retina, that was only attached at the papilla nervi optici and focally attached to the posterior side of the lens.

Within the chorioidea, partly covered by the ablated retina, there was a nodular round to oval shaped endophytic protruding soft mass (about 10 mm in diameter) located between the pars ciliaris of the ciliary body and the papilla nervi optici with a homogenously black colored cut surface.

Laboratory Results:
Urea: 1.499 mmol/l
Creatinin: 12906.692 µmol/l
Urea/Creatinin: 16
Alanin-amino-transferase (ALT): 500.1 nkat/l
Aspartat-amino-transferase (AST): 316.73 nkat/l
Alkaline phosphatase (ALKP): 316.73 nkat/l
Thyroxin: 25 nmol/l
Serum chemistry profile values were within normal limits.

Microscopic Description:
The conjunctiva bulbi, cornea, anterior eye chamber, irido-corneal angle, the lens and the nervus opticus / optic cup do not show any histological changes.

Limbus: The limbal cornea shows a mild infiltration by pigmented cells (melanosis oculi).
Iris: There is moderate mydriasis, the facies posterior contains multifocal single cysts.
Ciliary body: The outer non-pigmented epithelium reveals a mild to focally moderate atrophy.
Vitreous body: There is focal evidence of scattered plump melanin containing cells (questionable RPE).
Retina: A total retinal ablation with moderate to severe atrophy of all retinal layers (neuronal - inner/outer granular-and photoreceptor layer) is present.
Retinal pigmentary epithelium (RPE): There is focally mild hypertrophy.
Choroid: Located between ciliary body and papilla nervi optici, within the chorioid, there is a round to oval shaped, about 1 cm in diameter large chorioidal mass with focally infiltrative growth, partly covered by a thin layer of RPE and regular chorioidal pigmented cells (cream brown pigment). The cells are moderately densely packed, well demarcated and demonstrate solid to nodular growth pattern. The moderately pleomorphic cell population appears disordered, divided by a fine fibrovascular stroma. The cells are plump, round to weakly elongated with a diameter of about 25 µm, with eosinophilic cytoplasm with a variable content of cytoplasmatic granular, partly clumped brownish material (melanin granules) and often indistinct cell borders. Where discernible, the nuclei are about 10 µm in diameter and contain little condensed chromatin and one central nucleolus. Anisocytosis and anisokaryosis is high. Only few binucleated cells are visible, the bleached specimens show 0-1 mitotic figures per high power field. Focally, in the periphery of the cell proliferate there is a small area of osseous metaplasia.
Sclera: Opposing the tumor, the sclera is focal mildly thinned. There is no evidence of the neoplastic cells infiltrating the sclera.

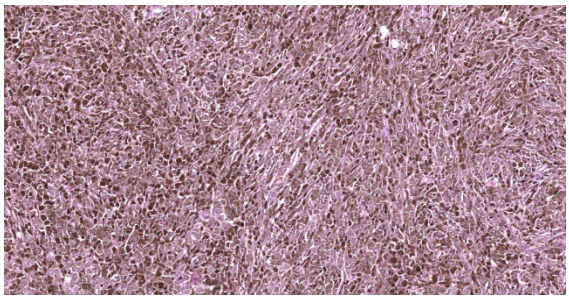

Figure 3-2. Globe, cat. Both polygonal to round and spindled melanocytes comprise the neoplasm. (HE, 132X)

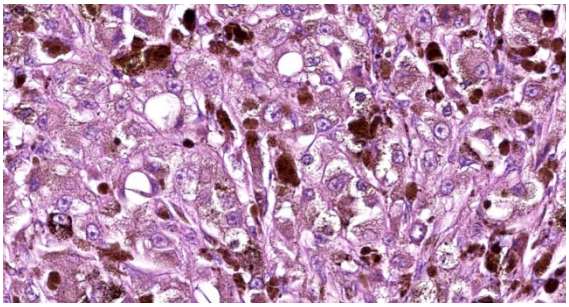

Figure 3-3. Globe, cat. Higher magnification of neoplastic in less pigmented areas demonstrate bland nuclei. (HE, 600X)

Contributor's Morphologic Diagnoses:

- Choroid: endophytic choroidal plump cellular melanoma
- Ciliary body: atrophy of outer non-pigmented epithelium, mild to focally moderate
- Retina: total retinal ablation and atrophy, moderate to severe
- RPE: hypertrophy, focal mild
- Iris: iridial mydriasis with focal cyst formation (facies posterior), focal, moderate
- Melanosis oculi, focal, mild

Contributor's Comment:
The most common melanocytic tumor in the eye of the cat is the feline diffuse iris melanoma.[2] In the present case the neoplastic cell proliferate was not involving the iridociliary body and it was only focal, protruding into the vitreous. Additionally, iridociliary epithelial tumor can also be pigmented, but have been ruled out in this case due to same reasons as mentioned above.[2]

According to Parul Singh and Abhishek Singh`s Paper in 2012, choroidal melanoma is the most common malignant primary neoplasia in humans with most often metastasis in liver, frequent the lung and bone.[6] Whereas canine choroidal melanomas are common, being usually benign and never metastasize[2], a choroidal melanoma has been reported in a cat the first time in 2011.[5] In the current case, no X-ray was performed to check for metastasis and no history of further locations with potential cell proliferates is known. The large cell proliferate led to ablation and atrophy of the retina with consecutive atrophy of the outer epithelium of the ciliary body and focal RPE hypertrophy, interpreted as secondary glaucomatous alterations.

Iridal cysts can be congenital or occur spontaneously, due to trauma or inflammatory processes.[3] In the current case, it is seen as an incidental finding just as the mild melanosis oculi.

Contributing Institution:
Institute of Veterinary Pathology Zuerich (IVPZ)
www.vetpathology.uzh.ch

JPC Diagnosis:
1. Eye: Choroidal melanocytoma.
2. Eye: Iridal cysts.

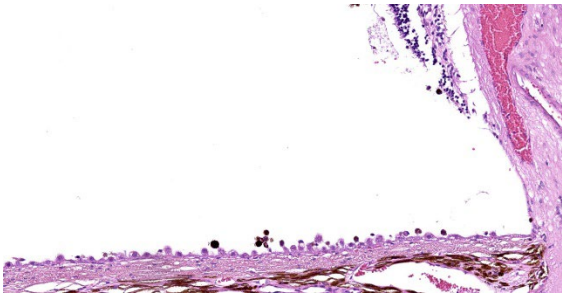

Figure 3-4. Globe, cat. There is hypertrophy of retinal pigmented epithelium. (HE, 1900X)

JPC Comment:
While iris melanoma is the most common intraocular tumor of cats, this case is an example of melanoma originating from extra-iridal structures, which is uncommon to rare in cats.[1,4] Only four cases of choroidal melanocytic neoplasms have been reported in the English literature. In two cases, neoplastic melanocytes infiltrated into the adjacent iris, and in a third case, there was a high mitotic rate (24 per 10 high power fields) with significant anisocytosis and anisokaryosis.[1] These three cases were diagnosed as choroidal melanoma.[1] The remaining case was diagnosed as a melanocytoma.[5]

Melanocytic neoplasms more commonly arise from the iris and are termed feline diffuse iris melanoma (FDIM).[4] These neoplasms start as iris melanosis, characterized as a non-neoplastic focus of proliferative and dysplastic melanocytes up to 3 layers thick.[4] Iris melanosis may remain static or rapidly progress to FDIM with infiltration of the subjacent iris stroma.[4] Early FDIM and iris melanosis are grossly indistinguishable, but as FDIM progresses, the iris becomes thickened and the pupil may be irregularly shaped and less mobile.[4] Features of malignancy for FDIM include a high mitotic rate (not well established and cut-off varies between studies), high nuclear to cytoplasmic ratio, significant nuclear pleomorphism, and multinucleation.[1,4] Survival for cats with FDIM is cor-

related with histologic invasion, with neoplasms confined to the iris or trabecular meshwork producing survival times similar to control cats, and neoplasms extending into the sclera associated with decreased survival time.[4] While cellular morphology can vary significantly and include patterns such as spindle cell, anaplastic, and giant cell variants, there is no correlation between morphology and metastasis.[4] Rates of FDIM metastasis vary from 19 to 63%, and the liver is the most common site of metastasis.[4] While some aggressive FDIMs metastasize quickly, others may metastasize late in the disease, sometimes years after the initial diagnosis.[4]

References:

1. Bourguet A, Piccicuto V, Donzel E, Carlus M, Chahory S. A case of primary choroidal malignant melanoma in a cat. *Vet Ophthalm*. 2015; 18(4): 345-349.
2. Dubielzig RR. Tumors of the Eye. In: Meuten DJ, ed. *Tumors in Domestic Animals*. 5th ed. Ames, IO: Wiley-Blackwell; 2017:892-911.
3. Gemensky-Metzler AJ, Wilkie DA, Cook CS. The use of semiconductor diode laser for deflation and coagulation of anterior uveal cysts in dogs, cats and horses a report of 20 cases. *Vet Ophthalmol*. 2004;7(5):360-8.
4. Kayes D, Blacklock B. Feline Uveal Melanoma Review: Our Current Understanding and Recent Research Advances. *Vet Sci.* 2022; 9(2): 46-59.
5. Semin MO, Serra F, Mahe V, Deviers A, Regnier A, Raymond-Letron I. Choroidal melanocytoma in a cat. *Vet Ophthalmol*. 2011;14(3):205-8
6. Singh P, Singh P. Choroidal melanoma. *Oman J Ophthalmol*. 2012; 5(1):3-9.

CASE IV:

Signalment:
1 year-old, intact female, Cavalier King Charles Spaniel, dog (*Canis familiaris*)

History:
This dog was a normal active puppy up until 4 weeks prior when the owner noted the puppy acting lethargic and had labored breathing. The puppy was brought to the vet and was diagnosed with a respiratory infection. Fungal cultures were negative. The puppy was started on an antibiotic, prednisone, and another medication (unknown). Clinical signs improved but then worsened and the puppy quickly died. All other puppies in the litter and dogs in the home were all normal with no clinical signs.

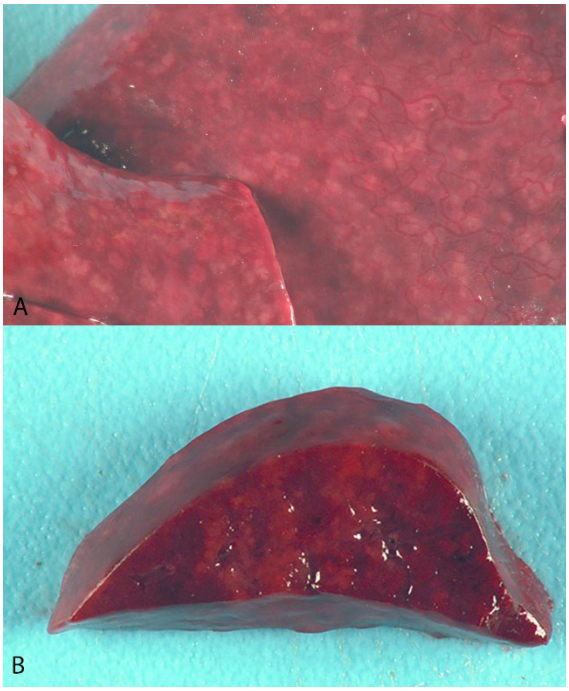

Figure 4-1. Lung, dog. The pulmonary parenchyma was diffusely dark red, rubbery, and did not collapse. There were hundreds of randomly scattered, 1-2 mm in diameter, tan to white, firm raised foci throughout all lung lobes. (Photo courtesy of: Michigan State University Veterinary Diagnostic Laboratory. Department of Pathobiology and Diagnostic Investigation - https://cvm.msu.edu/vdl) (HE, 5X)

Gross Pathology:
The pulmonary parenchyma was diffusely dark red, rubbery, and did not collapse. There were hundreds of randomly scattered, 1-2 mm in diameter, tan to white, firm raised foci throughout all lung lobes.

Laboratory Results:
No laboratory findings reported.

Microscopic Description:
Approximately 90% of alveolar spaces are multifocally expanded by eosinophilic, foamy, amorphous material with numerous approximately 7µm in diameter, teardrop-shaped, yeast structures that have variably thick walls highlighted by a Grocott's Methenamine Silver (GMS) stain. Moderate numbers of histiocytes are associated with these regions. The adjacent alveoli are lined by plump cuboidal type II pneumocytes. The remaining pulmonary parenchyma is extensively autolytic and contains multifocal mats of cadaver bacilli.

Contributor's Morphologic Diagnoses:
Lung: Severe, multifocal, histiocytic alveolitis with intralesional yeasts and type 2 pneumocyte hyperplasia

Contributor's Comment:
Pneumocystis sp., is a commensal yeast-like fungal organism, in the class Pneumocystidomycetes, found in the lungs of adult animals. Initial colonization with *Pneumocystis sp*. is thought to occur during the birthing process but can also be horizontally transmitted between the same species as an airborne organism[5,8]. Essentially every mammal has a unique strain of *Pneumocystis sp*. and interspecies transmission is not thought to occur. There are five host-specific *Pneumocystis sp*. that have been formally described in the literature and include: *P. carinii/wakefeldii* in rats, *P. murina* in mice, *P. oryctolagi* in rabbits, and *P. jirovecii* in humans[1]. Pneumocystis pneumonia (PCP) can occur in any species of animal, especially if immunocompromised. In humans, PCP and secondary airway obstruction are serious consequences in immunocompromised individuals, especially in those individuals that are infected with human immunodeficiency virus (HIV). *Pneumocystis* sp. are fastidious organisms and cannot be grown in continuous culture, leading researchers to heavily rely on animal models of disease[2,5,8]. *P. carinii* infections in rats were the original study models; however, due to host-specific genotypic and phenotypic variations, it was difficult to make comparisons to *P. jirovecii* infections in humans[2]. Additionally, due to the inability to recreate an HIV model in rats, rat models to study PCP infections were not ideal. Studies utilizing macaques infected with simian immunodeficiency virus (SIV) then became the most relevant animal model not only due to macaques developing clinical signs similar to

Figure 4-2. Lung, dog. Multiple sections of lung are submitted for examination. At subgross examination, all are consolidated with abundant foamy alveolar exudate. (HE, 5X)

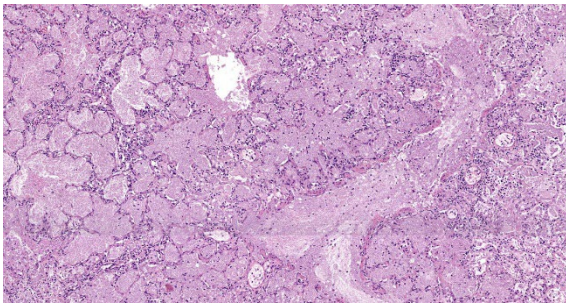

Figure 4-3. Lung, dog. Alveoli are filled with a foamy "soap-bubble" exudate; alveolar septa are expanded by macrophages, fibrin, and edema. (HE, 100X)

those in humans with AIDS, but *P. carinii* derived from humans and non-human primates are evolutionarily more related than *P. carinii* derived from rats[2].

Pneumocystis pneumonia, suspected to be caused by *Pneumocystis carinii f sp. canis*[6] is uncommon in dogs. Young to middle-aged Cavalier King Charles Spaniels and Miniature Dachshunds are overrepresented and may have inheritable immunodeficiency predisposing them to over colonization[3,9]**.** In a study that evaluated IgG, IgM, and IgA serum concentration in Cavalier King Charles Spaniels diagnosed with Pneumocystis pneumonia compared to breed and age-matched nonaffected dogs, it was found that affected dogs had significantly lower IgG concentrations[9]. These dogs tend to respond to medical treatment if treated early in the course of the disease.

Pneumocystis infects hosts by direct attachment to the alveolar epithelium via surface antigen glycoprotein A (gpA). The life cycle is composed of two morphologically distinguished forms, a trophic form and a cystic form which undergo binary fission and sexual replication, respectively. The trophic form is the predominant form during infection and is characterized by 1-4µm, thin-walled, uninucleate organisms[8]. The cystic form is 5-8 µm in diameter, thick-walled, and contains 8 intracystic nuclei/bodies. The intracystic bodies are released, attach to type I pneumocytes, and are thought to develop into the trophic form[4].

Pneumocystis can evade host immunity due to its cell wall composed of mannose-rich polysaccharides and heavily glycosylated surface antigens[4]. gpA is the key surface antigen responsible for attachment to the host epithelium as well as evasion of host immunity via interactions with macrophages, surfactant proteins, and fibronectin[4]. Multiple genes encode this protein; however, during infection only one isoform is expressed[3]. The expression of this isoform is unique to the associated organism adapted to each host species. Pneumocystis causes disease by expanding alveoli as well as possibly altering surfactant homeostasis. Infection is controlled by macrophages and cell-mediated immunity[4].

Gross lesions can be multifocal to diffuse and are often characterized by red to brown areas of consolidation that may be variably nodular[4]. Histologically, lesions are characterized by foamy eosinophilic material and variable numbers of foamy macrophages that fills alveolar spaces. Organisms are difficult to identify on routine hematoxylin and eosin staining. Special staining with methenamine sliver highlights the walls of the organism. Secondary, variably prominent findings include, increased interstitial lymphocytes, plasma cells, and type II pneumocyte hyperplasia[4]. The number of organisms within alveolar spaces can greatly vary, thus PCR is the most sensitive detection method.

Contributing Institution:
Michigan State University Veterinary Diagnostic Laboratory. Department of Pathobiology and Diagnostic Investigation - https://cvm.msu.edu/vdl

JPC Diagnosis:
Lung: Pneumonia, interstitial, histiocytic and

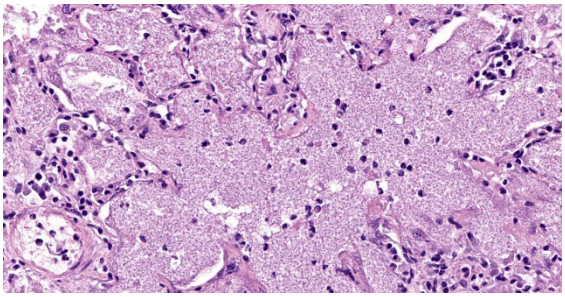

Figure 4-4. Lung, dog. High magnification of the characteristic alveolar exudate characteristic of infection with Pneumocystis carinii. (HE, 450X)

necrotizing, diffuse, marked, with type II

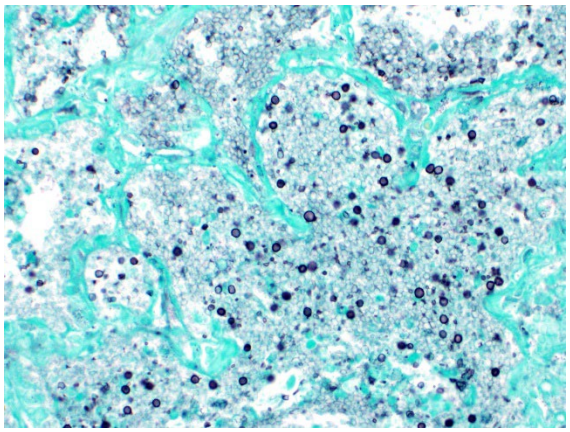

Figure 4-5. Lung, dog. A silver stain demonstrates cysts of Pneumocystis carinii within the alveolar exudate. (HE, 450X)

pneumocyte hyperplasia and many intra-alveolar yeasts.

JPC Comment:

The contributor provides a great overview of this ubiquitous fungus which can infect a wide variety of hosts. A recent meta-analysis evaluated the clinical and diagnostic features of 43 dogs with pneumocystosis.[10] Miniature dachshunds and cavalier King Charles spaniels were predisposed.[10] Clinical signs were nonspecific and included weight loss, cough, dyspnea, and cyanosis, but, interestingly, most dogs had normal body temperature. [10] Hemogram changes include leukocytosis and neutrophilia.[10] The authors found that hypogammaglobulinemia was useful in the diagnosis and reflects the inability of infected dogs to class-switch from IgM to IgG production.[10] On necropsy, the lungs were firm or rubbery and discolored or pale. [10] Pneumothorax was uncommonly seen in these dogs but is a common finding in human infections.[10] Cytologic examination of bronchoalveolar lavage fluid, the mainstay of diagnosis in humans, was insensitive and unreliable in this report; more sensitive antemortem diagnostics included fine needle aspirates of the lung and cytologic examination of tracheal swabs.[10] Histologic findings included lymphohistiocytic interstitial pneumonia with type II pneumocyte hyperplasia and foamy to granular eosinophilic material filling alveolar lumens containing poorly-staining extracellular and intracellular trophozoites and cysts.[10] GMS and PAS highlighted the cyst walls and confirmed the diagnosis.[10] Advanced diagnostics that were useful in the meta-analysis include PCR, electron microscopy, and immunohistiochemistry.[10]

An uncommon complication of pneumocystis infection is disseminated spread, which was recently reported in a young adult toy poodle.[7] In addition to the alveolar lumen, the fungus was found in the pulmonary interstitium and had spread to multiple lymph nodes, the liver, heart, spleen, pancreas, kidneys, and gastrointestinal tract.[7] There was marked lymphoid depletion in multiple lymph nodes and the spleen.[7] Based on the distribution pattern, the authors speculated that the fungus spread through lymphatics.[7] The dog may have been immunodeficient due to a prolonged course of corticosteroids or due to a underlying immunodeficiency.[7]

Conference participants discussed the gross photograph from this case; the pale patchy discoloration combined in an immunosuppressed animal (i.e. in a severe combined immunodeficiency in an Arab foal, or an NHP infected with SIV) is strongly suggestive of *Pneumocystis* pneumonia.

References:

1. Alanio A, Bretagne S. Pneumocystis jirovecii detection in asymptomatic patients: what does its natural history tell us? *F1000 Research*. 2017; 6.
2. Board KF, Patil S, Lebedeva I, et al. Experimental Pneumocystis carinii pneumonia in simian immunodeficiency virus–infected rhesus macaques. *J Infect Dis.* 2003;187(4): 576-588.
3. Farrow, BRH, Watson, ADJ, Hartley, WJ, and Huxtable, CRR. Pneumocystis

pneumonia in the dog. *J Comp Path*. 1972; 82(4): 447-453.
4. Maxie, MG. *Jubb, Kennedy & Palmer's Pathology of Domestic Animals*. Vol 2. Elsevier. 2015; 535-536.
5. Morris A, Sciurba FC, Norris KA. Pneumocystis: a novel pathogen in chronic obstructive pulmonary disease? *COPD*. 2008;(1)5: 43-51.
6. Ralph E, Reppas G, Halliday C, Krockenberge M, Malik R. Pneumocystis canis pneumonia in dogs. *Microbiology Australia*. 2015; 36:79-82.
7. Sakashita T, Kaneko Y, Izzati U z, et al. Disseminated Pneumocystosis in a Toy Poodle. *J Comp Pathol.* 2020; 175: 85-89.
8. Thomas C, Limper A. Current insights into the biology and pathogenesis of Pneumocystis pneumonia. *Nat Rev Microbiol*. 2007;5: 298–308.
9. Watson PJ, Wotton P, Eastwood J, Swift ST, Jones B, Day MJ. Immunoglobulin deficiency in Cavalier King Charles spaniels with Pneumocystis pneumonia. *J Vet Intern Med*. 2006; 20(3): 523-527.
10. Weissenbacher-Lang C, Fuchs-Baumgartiner A, Guija-De-Arespocachaga, Klang A, Weissenbock H, Kunzel F. Pneumocystosis in dogs: meta-analysis of 43 published cases including clinical signs, diagnostic procedures, and treatment. *J Vet Diagn Invest*. 2018; 30(1): 26-35.